Journal of the Serbian Society for Computational Mechanics / Vol. 17 / No. 2, 2023 / pp 38-54
(10.24874/jsscm.2023.17.02.04)

NUMERICAL STUDY OF MECHANICAL BEHAVIOR OF REPAIRED INCLINED CRACKED UNDER COMPLEX SHEAR-SHEAR LOAD: PERFORMANCE AND DURABILITY OF ALUMINUM 2024-T3 PLATE

Ahmed Allem[1*], Mokadem Salem[1], Sofiane Talbi[1,2] and Abderahmane Sahli[1]

[1] (LMPM) Laboratory of Mechanics and Physics of Materials, Department of Mechanical Engineering, University of Sidi Bel Abbes 22000, Algeria
e-mail: allem.ahmed92@gmail.com, moka_salem@yahoo.fr, sahliabderahmen@yahoo.fr
[2] (LAPS) Laboratory of Aeronautics and Propulsive Systems, University of USTO 31000, Algeria
e-mail: sfianew100@gmail.com
**Corresponding author*

Abstract

In this study, a finite element model was developed to analyze the mechanical behavior of repairing aluminum 2024-T3 structures subjected to complex shear-shear loads using composite patch repair techniques. The study aimed to investigate the effect of different patch sequences on the mechanical behavior of the repaired structure, including the orientation of the fiber patch, to improve durability under complex shear-shear loading conditions. The study demonstrated that the FEM approach is a robust and precise method for optimizing patch repair and studying the effect of mechanical loads on patch repair effectiveness for aluminum 2024-T3 structures.

Keywords: complex shear loading, crack, finite element modelling, patch repair.

1. Introduction

Alan Baker (1984) was one of the pioneers in the development of bonded composite repairs for metallic structures. Bonded composite repairs have emerged as a valuable solution for extending the life of aircraft structures over the past twenty years, providing an efficient means of restoring the ultimate load capability of the repairing structure (Alan Baker 1995). In the past two decades, the field of manufacturing and advanced technology has widely developed and utilized composite material technology (Ibrahim et al. 2018 and Atluri et al. 1997).

One effective method of increasing the lifespan of aerial and marine structures involves using composite repairs in conjunction with metal structures. The benefits of using composite materials include reducing the stress intensity factor at the crack tip, improving fatigue behavior, increasing performance, and lowering the likelihood of failure, all of which enhance the durability of damaged structures (Chow, 1997). Benyahia and colleagues (Benyahia et al. 2014) investigated the adhesive integrity damage that may occur during aircraft composite structure repair utilizing various repair techniques (Salem et al. 2018; Salem et al. 2021; and M. Berrahou et al. 2017). They studied the effect of the stress intensity factor (SIF) on cracking and corrosion. Chakherlou and colleagues (Chakherlou et al. 2012) discussed an experimental investigation into the effect

of cold expansion on the fatigue life improvement of aluminum alloy 2024-T3 plates used in double-shear lap joints. The effectiveness of composite patch repairs depends on various parameters, such as the geometrical and mechanical properties of the patch and adhesive layer. Researchers have been exploring different patch shapes to optimize the repair process. Bouchiba et al. (2016) used a static approach to study the effect of the patch and concluded that the butterfly shape reduces failure energy at the crack tip and minimizes shear stresses in the adhesive layer. Mhamdia et al. (2012) proposed a new patch method called the "patch double arrow," which was found to be more efficient than the conventional rectangular shape in terms of normal tension stress relaxation and crack head concentration (Chung et al. 2003 and Jeong et al. 2000).

Salem and colleagues (Salem et al. 2021) analyzed the efficiency of the patch from the perspective of fracture mechanics and disbanding of the patch. They developed a composite patch that led to a maximum reduction of the stress intensity factor. The findings of these studies suggest that optimizing the composite patch is a crucial factor in ensuring the effectiveness of composite patch repairs. Mechab B et al. (2020) showed that crack propagation can occur in many structural components. They are the cause of premature damage in structures. The fracture prediction and the reliability of structure in various practical applications are primordial given their impact on the economic plan and security. A. Benkheira et al. (2022) conducted a study using three-dimensional finite element numerical analysis to investigate the performance of plates repaired by composite patches.

Based on the previous studies, our study developed a finite element model to analyze the effectiveness of repairing a metallic structure subjected to complex shear-shear loads using composite patch repair techniques. The study aims to investigate the effect of different patch sequences on the mechanical behavior of the repaired structure, including the different orientations of the fiber patch, to enhance durability under complex shear-shear loading conditions. The developed finite element model is used to simulate the behavior of the repaired structure, considering different patch sequences and material properties of the composite patch and adhesive layer. The analysis results provide valuable insights into the optimal design of composite patch repair techniques for AL 2024-T3 structures subjected to complex shear-shear loads to enhance the performance and durability of these structures.

2. Geometrical model

The geometrical composite patch repair plate in Fig. 1 is crucial in analyzing the mechanical behavior of the plate. It helps in understanding how the plate responds to complex shear-shear loads under σ_x=100MPa and σ_y=150 MPa. The plate is made of 2024-T3 aluminum and has a crack with an inclined length of 2a = 62mm, which is rectified by applying boron epoxy composite patches in eight distinct stacking sequences on the plate's surface. To affix these patches to the plate, FM 73 adhesive is used for its adhesive properties.

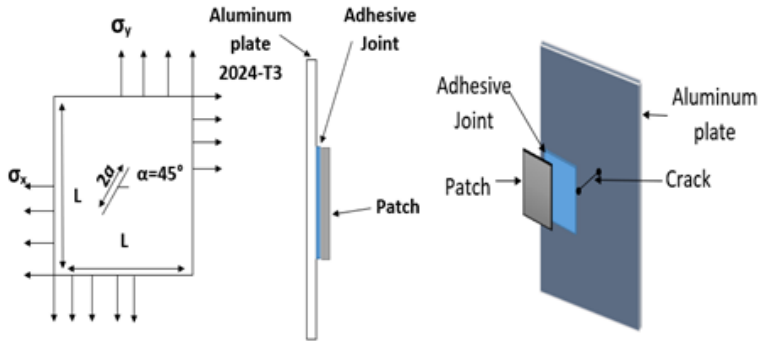

Fig. 1. Geometrical model

3. Mechanical properties

Table 1 provides indispensable insights into the dimensions and mechanical characteristics of Aluminum 2024- T3, composite patches and the adhesive substances employed in the repair process. It underscores the paramount importance of precise alignment during the patch application, ensuring a secure and robust attachment to the plate. This precision is essential for enabling the composite patch to withstand and effectively respond to the demanding complex shear-shear loads to which it is subjected.

Properties	Material l	Material 2	Material 3
	(Plate) Aluminum 2024- T3	(Composite patch) Boron/epoxy	(Adhesive) (FM-73)
Length (mm)	250	50	50
Width (mm)	250	50	50
Thickness (mm)	2	2	0.2
E1 (MPa)	72000	208000	2550
E2 (MPa)	-	25000	-
E3 (MPa)	-	25000	-
ν12	0.33	0.21	0.32
ν13	-	0.21	-
ν23	-	0.21	-
G12(MPa)	-	7200	-
G13(MPa)	-	5500	-
G23(MPa)	-	5500	-

Table 1. Mechanical properties of the materials used.

4. Validation of the model

4.1. Analytical method

In the field of stress intensity factor (SIF) analysis, it is critical to delve into the distinct modes of behavior exhibited by cracks. Specifically, when we focus on Mode I loading, we are addressing a situation where the applied load acts perpendicular to the crack planes.

Mode I, Mode II and Mode III are fracture modes that describe different types of crack growth and deformation in materials. These fracture modes are often used to characterize the behavior of materials under different loading conditions. The modes are defined based on the relative motion of the two sides of a crack and the direction of the applied force.

Mode I (Opening Mode or Tensile Mode):

In the context of fracture mechanics, the phenomenon of crack opening, specifically observed in Mode I fracture, is characterized by the primary crack propagation occurring normal to the plane of the crack faces. This mode of fracture induces an opening or tensile separation within the material, wherein the applied force acts perpendicular to the crack surfaces, compelling the crack to widen. This loading condition accentuates the extension of the crack along its length, emphasizing the tensile nature of the stress state and the subsequent material separation caused by the forces applied in this specific direction.

$$KI = Y\sigma\sqrt{(\pi a)} \tag{1}$$

$$\sigma_x = \frac{K_1}{\sqrt{2\pi r}} cos\frac{\theta}{2}\left[1 - sin\frac{\theta}{2}sin\frac{3\theta}{2}\right] \tag{2}$$

$$\sigma_y = \frac{K_1}{\sqrt{2\pi r}} cos\frac{\theta}{2}\left[1 + sin\frac{\theta}{2}sin\frac{3\theta}{2}\right] \tag{3}$$

$$\tau_{xy} = \frac{K_I}{\sqrt{2\pi r}} sin\frac{\theta}{2}cos\frac{\theta}{2}cos\frac{3\theta}{2} \tag{4}$$

Mode II (Sliding Mode or In-Plane Shear Mode):

In the realm of fracture mechanics, the phenomenon known as crack sliding is prominently observed in Mode II fracture. In this mode, the principal mechanism of crack propagation entails the sliding or shearing of one side of the crack in relation to the other. This sliding motion is the result of loading conditions where the applied force acts parallel to the plane of the crack surfaces, inducing a lateral displacement or shear between the crack faces. The loading scenario in Mode II accentuates the propensity of the material to resist shear forces, highlighting the importance of understanding and characterizing this specific mode of fracture for a comprehensive comprehension of material behavior under different loading conditions.

$$\sigma_x = -\frac{K_{II}}{\sqrt{2\pi r}} sin\frac{\theta}{2}\left[2 + cos\frac{\theta}{2}cos\frac{3\theta}{2}\right] \tag{5}$$

$$\sigma_y = \frac{K_{II}}{\sqrt{2\pi r}} sin\frac{\theta}{2}cos\frac{\theta}{2}cos\frac{3\theta}{2} \tag{6}$$

$$\tau_{xy} = \frac{K_{II}}{\sqrt{2\pi r}} cos\left[1 - sin\frac{\theta}{2}sin\frac{3\theta}{2}\right] \tag{7}$$

Mode III (Tearing Mode or Antiplane Shear Mode):

In the distinctive fracture mode identified as Mode III, often referred to as Tearing Mode or Antiplane Shear Mode, the predominant mechanism of crack propagation is characterized by tearing or antiplane shear deformation. In this mode, the material experiences a tearing phenomenon where one side of the crack is displaced relative to the other, resulting in a shear deformation perpendicular to the plane of the crack faces. The loading condition specific to Mode

III involves the application of force tangentially to the crack surfaces. This tangential force induces tearing or shear deformation, emphasizing the lateral displacement and antiplane shear nature of the fracture mode. The understanding of the intricacies of Mode III is crucial for a comprehensive grasp of material response under such loading conditions, providing valuable insights into the material's resistance to tearing and shear forces.

$$\tau_{xz} = -\frac{K_{III}}{\sqrt{2\pi r}} sin\frac{\theta}{2} \tag{8}$$

$$\tau_{yz} = \frac{K_{III}}{\sqrt{2\pi r}} cos\frac{\theta}{2} \tag{9}$$

$$\sigma_x = \sigma_y = \sigma_z = \tau_{xy} = 0 \tag{10}$$

In the general case (involving all three modes), the stress field takes the following form:

$$\sigma_{ij}(\theta) = \frac{1}{\sqrt{2\pi r}}\left[K_I f_{ij}^{I}(\theta) + K_{II} f_{ij}^{II}(\theta) + K_{III} f_{ij}^{III}(\theta)\right] \tag{11}$$

The functions $f_{ij}^{I,II,III}$, are functions that depend solely on the polar angle θ. In the crack plane (θ = 0), these functions reduce to:

$$f_{22}^{I}(\theta) = f_{12}^{II}(\theta) = f_{23}^{III}(\theta) = 1 \tag{12}$$

KI, KII, and KIII are the stress intensity factors for Mode I, Mode II, and Mode III, respectively. It is evident, therefore, that the stress field exhibits a singularity at the crack tip.

$$\left(\frac{1}{\sqrt{r}}\right) \tag{13}$$

K1 quantifies the propensity for crack growth in materials subjected to Mode I loading, providing a crucial insight into their fracture behavior. Another fundamental element in the equation (1) is 'Y,' a parameter or function that embodies various factors, including crack geometry and shape. 'Y' is indispensable for precisely determining the Stress Intensity Factor in Mode I loading scenarios, allowing for a comprehensive evaluation of crack behavior.

The parameter '*σ*' represents the applied stress on the material, indicating the magnitude of the mechanical load being exerted on a given component or structure. 'a', on the other hand, stands for the characteristic length or size of the crack. This dimension is of paramount importance as it governs the crack dimensions and its influence on stress distribution within the material. Lastly, the term 'πa' encompasses the square root of π (pi) multiplied by the crack size 'a.' This term serves as a critical factor in the equation, capturing the size of the crack and its direct correlation with the Stress Intensity Factor. These components collectively form the foundation of stress intensity factor calculations, enabling engineers and scientists to predict and mitigate the risk of crack propagation in various mechanical systems and materials

According to the findings, analytical validation presented by Rose and colleagues (1981) in the equation (1), a fundamental and widely accepted relationship exists between the applied stress (σ) on the plate and the corresponding stress intensity factor (SIF). Fig. 2 gives the analytical validation of the mode l of serves as a fundamental tool in Mode I loading analysis, enabling researchers to quantify the relationship between applied stress, crack geometry, and the resulting stress intensity factor. It is invaluable in predicting and understanding how cracks respond to Mode I loading conditions, which is of paramount importance in fracture mechanics and materials engineering.

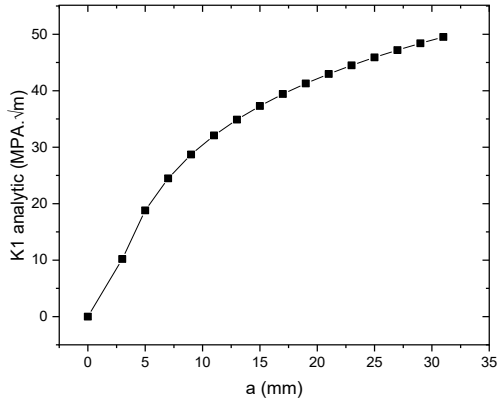

Fig. 2. Analytical validation of the model

4.2. New approximation method for SIF calculation in a case of cracks (Numerical method)

The process of meshing with computational software (Abaqus Simulia 2014) involves selecting the appropriate element type and size, and defining the appropriate element connectivity, based on the geometry and loading conditions.

Fig. 3 shows a structured mesh is made up of regularly shaped elements that follow a consistent pattern, while a structured mesh is made up of elements of varying shapes and sizes that conform to the geometry more closely. In addition to selecting the appropriate mesh type, one must ensure that the mesh has sufficient density to capture the complex behavior of the structure. Overall, the quality of the mesh is a critical factor in achieving accurate and reliable simulation results, and careful attention must be given to this step of the analysis process.

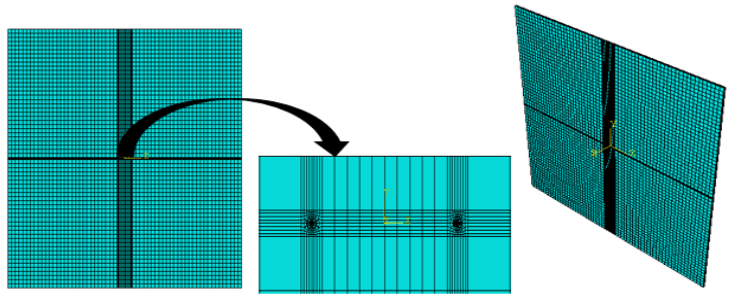

Fig 3. Meshing of the center crack mode I

The numerical validation of Stress Intensity Factor (SIF) Fig.4, is a critical parameter in understanding the stress and strain state of the crack head, and thus, it is essential to accurately calculate it for the model to be reliable. Meshing is a critical step in finite element analysis, as it involves dividing the geometry into smaller elements to enable numerical simulations. The quality of the mesh has a significant impact on the accuracy and reliability of the simulation results.

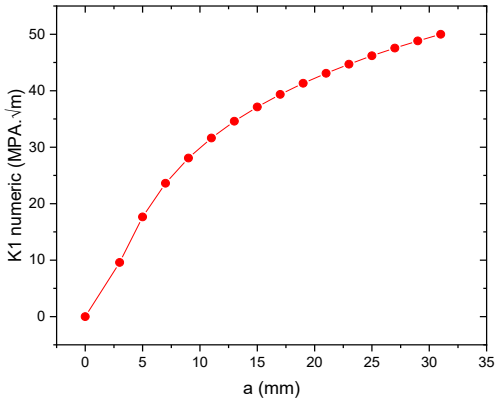

Fig. 4. Numerical validation of the model

4.3. The comparative analytical-numerical validation of the model

Fig. 5 presents a comparison between analytical and numerical results for the stress intensity factor 'k1. What stands out is the remarkable consistency between the two sets of values throughout the entire dataset. This high level of agreement suggests that the numerical approach employed for calculating 'k1' is robust and accurate, aligning closely with the predictions from the analytical method. As 'k1' values consistently increase with the progression of the dataset, it indicates a clear relationship between a parameter or condition and stress intensity, where precise stress factor predictions are paramount for ensuring structural integrity and safety. The close correspondence between analytical and numerical results underscores the reliability of computational simulations, emphasizing the importance of quality assurance in numerical models for practical engineering and scientific applications. In practical terms, Fig. 5 provides valuable insights for engineers and researchers, enabling them to make informed decisions when assessing the structural behavior of materials and components under varying conditions.

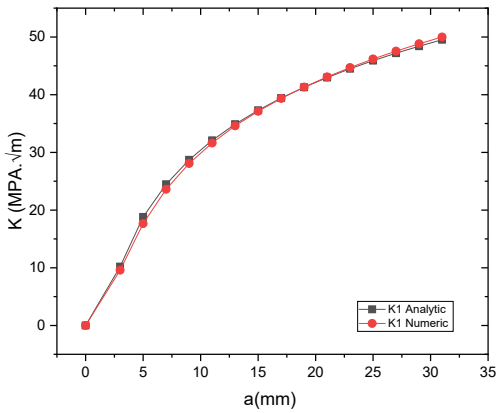

Fig. 5. The analytical-numerical validation of the model

5. The analysis of mechanical behavior using FEM

The FEM model was based on the panel configuration tested by Luzar (1997). The 2024-T3 panel was manufactured and tested to determine the fatigue crack growth values of the aircraft cell structure. The panel thickness and lengths were selected to mimic the configuration of a real aircraft structure. The test panels were held by gripping end fixations, which resulted in the transmission of all test loads through friction of the joints. The loading was arranged to produce uniform stresses and displacements throughout the test section. The use of C3D8 elements, specifically 8-node linear bricks, based on fracture mechanics and finite element modeling is a highly effective method for modeling the structure of a repair patch.

The mesh used in Fig. 6 is based on the finite element method and is depicted, which clearly illustrates the shape of the 2024-T3 patch. The stress intensity factor value (SIF) was determined using the domain integration method in (Abaqus Simulia software 2014). This method is renowned for providing a high level of accuracy for rough 3D models. For all structures, a regular grid was used, with a total of 30683 elements for the repair structure, 9820 for the patch, and 2800 for the adhesive. To account for the geometric singularities caused by the inclined crack in the center of the plate, the mesh was refined around the crack. This refinement remained unchanged throughout the calculation process to avoid any influence on the results. By connecting the nodes of the elements, a perfect connection between slabs and interlocking paving was created. This ensured that the structure and the composite sheet had the same mesh, thereby providing a consistent and reliable mode I.

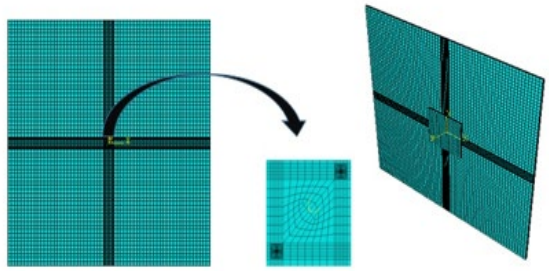

Fig. 6. Meshing of the study model

6. Results and discussion

In this study, we conducted a comprehensive investigation of the mechanical behavior of aluminum alloy 2024-T3. The simulation results reveal a clear correlation between strain and stress within the material. As the applied strain increases from 0 to 0.25, we observed a corresponding increase in stress, ranging from 0 MPa to 681.075 MPa. Fig. 7 provides valuable insights into the material's deformation characteristics, demonstrating its ability to withstand substantial loads before reaching its ultimate tensile strength. The stress-strain relationship is notably linear within this range, indicating that aluminum 2024-T3 maintains its mechanical integrity under various loading conditions, making it a suitable choice for applications where both strength and lightweight properties are crucial. These findings contribute to a deeper understanding of the material's behavior and can inform the design and engineering of structures and components utilizing aluminum 2024-T3.

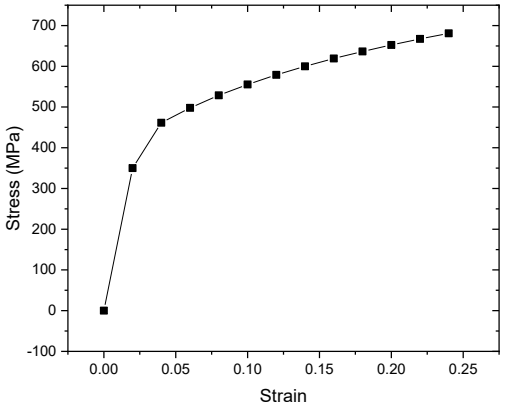

Fig. 7. Stress-strain curves for aluminum 2024-T3

6.1. Boundary condition

In the realm of aluminum plate research, particularly in the context of 2024-T3 alloy, boundary conditions play a crucial role when subjected to shear-shear loading. These conditions define how the material interacts with its surroundings, influencing the deformation and stress distribution within the plate. In shear-shear loading scenarios, it is essential to carefully consider the boundary conditions to accurately simulate real-world applications and predict the behavior of the 2024-T3 aluminum plate. By precisely defining these conditions, Fig. 8 can help us gain insight into how this high-strength alloy responds to complex loading conditions patch reparation, aiding in the development of innovative designs and materials for a variety of aerospace and structural applications.

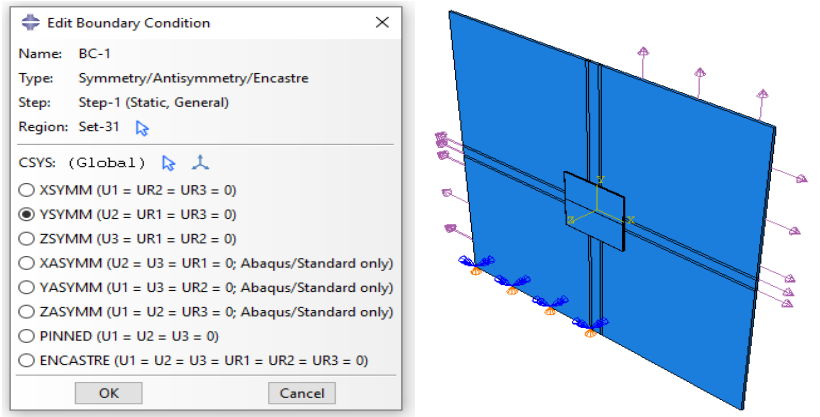

Fig. 8. Boundary condition of the model

6.2. Performance study and Durability

Table 2 presents the different composite patch stacking sequences for optimal use in crack repair. This optimal use is obtained when one manages to select, in a judicious way, the type of stacking sequence allowing the reduction of the stress intensity factor in mixed mode as much as possible.

The orientation of the fiber patch is assumed different. The results show that the repair by composite patch of sequence [A] leads to a very low fracture at the crack tip compared to the sequence [B] and [C]. This reduction is very significant and can exceed 80% when the folds are oriented in sequence [A]. To confirm this observation, we compare the fracture at the crack tip in mixed mode and in different way like max stress and max shear in adhesive.

Case	Stacking sequences
[A]	[00°/45°/-45°/90°/90°/45°/-45°/00°]
[B]	[90°/45°/-45°/00°/00°/45°/-45°/90°]
[C]	[45°/90°/-45°/00°/00°/-45°/90°/45°]

Table 2. The different cases of patch stacking sequences

Fig. 9 provides valuable insights into the relationship between the number of elements (Nb of elements) and the stress levels (σ) in a finite element modeling scenario, particularly in the context of unrepaired and repaired sequences [A], [B], and [C]. The stress values are measured in (MPa). As the number of elements increases, there are notable trends in stress levels. In the unrepaired condition, where no repair sequences have been applied, the stress (σ) is at its highest when the number of elements is at its lowest (600 elements). This suggests that with fewer elements, the structural analysis may yield higher stresses, possibly due to less refined modeling. However, as the number of elements increases, the stress levels decrease significantly. This decrease indicates that a finer mesh with more elements provides a more accurate representation of the structural behavior, resulting in lower stresses. When considering the repaired sequences, [A], [B], and [C], a similar trend is observed. The application of repair sequences generally results in lower stress levels compared to the unrepaired condition. This signifies that the repairs effectively reduce the stress concentrations within the structure. Additionally, Fig. 9 shows that the magnitude of stress reduction varies with the number of elements and the specific repair sequence applied. For example, in the case of repair sequence [A], the stress reduction is noticeable, and it continues to decrease as the number of elements increases.

These findings underscore the importance of the finite element modeling approach and the role of the number of elements in accurately predicting stress levels in structural analysis. Moreover, Fig. 9 demonstrates the positive impact of repair sequences in mitigating stress concentrations, which is crucial for optimizing the structural performance and safety of engineering components. Researchers and engineers can use these data to make informed decisions regarding the mesh refinement and the effectiveness of repair strategies in various structural scenarios.

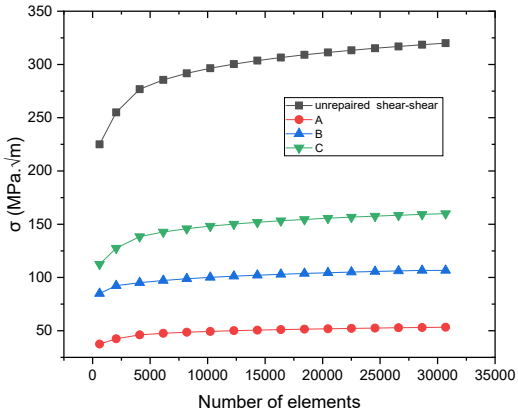

Fig. 9. Variation of max stresses vs number of elements under different stacking sequences

Fig. 10 presents a comprehensive comparison between unrepaired and repaired shear-shear conditions, with a particular focus on the stress intensity factor K1, measured in (MPa. √m). This dataset offers valuable insights into the effectiveness of repair sequences denoted as [A], [B], and [C]. In the unrepaired shear-shear condition, the K1 values initially start at zero, which is expected since no repairs have been implemented at this stage. As we move through the dataset, we observe a substantial increase in K1 values for all repaired sequences, indicating the positive impact of repairs on the structural integrity. Repaired sequence [A] shows a gradual but consistent increase in K1 values, suggesting that this particular repair sequence is effective in enhancing the material's resistance to shear forces. Repaired sequences [B] and [C] also exhibit similar trends, with the K1 values increasing steadily over the course of the dataset. The varying rates of increase among the repaired sequences may reflect differences in repair materials or methodologies used. The observed results highlight the potential of repair patches to strengthen structures under shear-shear conditions. These repairs appear to be particularly effective, as evidenced by the notable increase in K1 values. Further analysis and interpretation of these data could provide valuable guidance for optimizing repair strategies and materials, ultimately contributing to the advancement of repair patch technology in the field of structural mechanics. Moreover, these data underscore the significance of proper repair procedures in enhancing structural integrity, an essential consideration in maintaining the safety and longevity of various engineering structures.

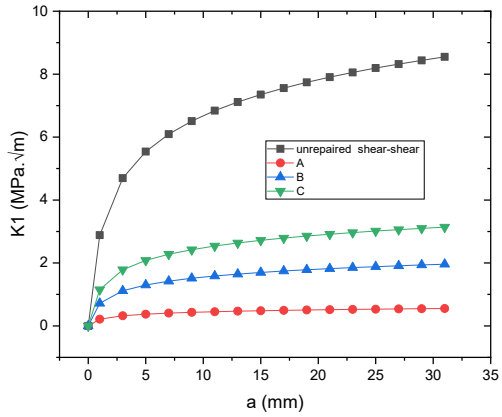

Fig. 10. Variation of SIF (K1) different stacking sequences

Building upon the previous discussion of stress intensity factor K1, Fig. 11 further delves into the mechanics of repair patches, focusing on K2, also measured in (MPa. √m). Like K1, K2 plays a crucial role in assessing structural integrity, especially in shear-shear conditions. However, as we progress through the data, it becomes evident that the repairs, represented by sequences [A], [B], and [C], have a noticeable impact on K2 as well. K2 observed in Fig. 11 are somewhat analogous to those seen in K1. Repaired sequence [A] exhibits a consistent increase in K2 values, indicating an enhancement in material resistance to shear forces. Similarly, repaired sequences [B] and [C] also display rising K2 values, though at different rates. The correlation between K1 and K2 is notable. In the context of repair patch mechanics, the concurrent increase in both K1 and K2 implies that the applied repairs are effective not only in strengthening the material against tensile forces (K1), but also in enhancing its resistance to shear forces (K2). This suggests a comprehensive improvement in structural performance, which is a crucial consideration in engineering and materials science, particularly for structures subjected to complex loading conditions.

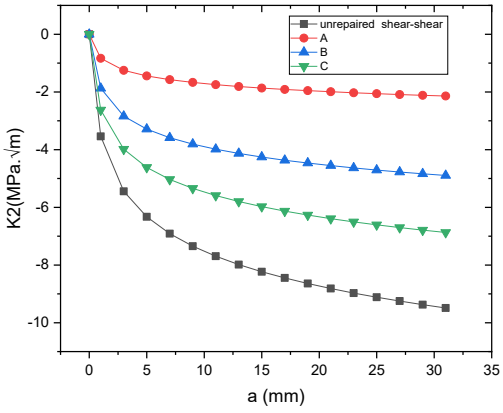

Fig. 11. Variation of SIF (K2) different stacking sequences

In summary, K2 reinforces the significance of repair patches in augmenting structural integrity under shear-shear conditions. The close relationship between K1 and K2 underscores the holistic nature of the repairs, emphasizing their positive impact on both tension and shear resistance. This dual improvement aligns with the broader goal of ensuring the safety and longevity of engineering structures, making it a valuable contribution to the field of repair patch mechanics.

6.3. Adhesive behavior study

In the evaluation of FM-73 adhesive behavior, Fig. 12 illustrates the relationship between strain percentage and stress. As strain percentage increases from 0 to 7.87%, the stress applied to the adhesive gradually rises from 0 to 57.05%. This data suggests that FM-73 adhesive exhibits a nonlinear stress-strain behavior, with an initial region of relatively low stress up to 1.46% strain, followed by a steeper increase in stress between 1.46% and 7.87% strain. Such behavior is typical of many adhesive materials, and it is essential to understand this stress-strain response for practical applications, such as in structural bonding or material reinforcement, where adhesive strength under specific strain conditions is crucial. Further investigation and analysis may be necessary to fully characterize the adhesive's mechanical properties and determine its suitability for specific engineering applications.

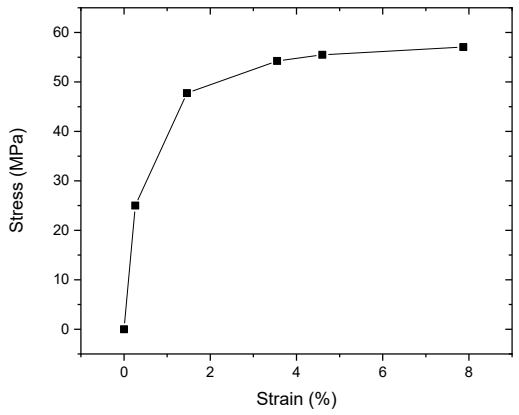

Fig. 12. Stress-strain curve of the FM 73 epoxy adhesive

In the investigation of FM-73 shear adhesive's performance under shear-shear loading conditions, the recorded data in Fig. 13 reveals an intriguing pattern in the maximum shear stress values in (xy) plane across three distinct loading sequences, denoted as [A], [B], and [C]. Starting with sequence [A], the initial maximum shear stress is observed at approximately 1.42 MPa, and as the loading continues, it steadily increases, culminating at nearly 2.00 MPa. Sequence [B], on the other hand, initiates with a slightly higher shear stress of around 2.84 MPa and exhibits a similar progressive increase, reaching approximately 4.00 MPa. Interestingly, sequence [C] demonstrates the highest initial maximum shear stress, commencing at approximately 4.26 MPa, and maintains a consistent pattern of growth throughout the loading process, ultimately achieving a value close to 6.00 MPa. These data underscore the significant influence of the loading sequence on the FM-73 adhesive's shear strength, with sequence [C] exhibiting the highest shear resistance, followed by sequence [B] and then sequence [A]. Further investigation is needed to discern the

underlying factors contributing to these varying shear behaviors and to optimize the adhesive's performance for specific applications.

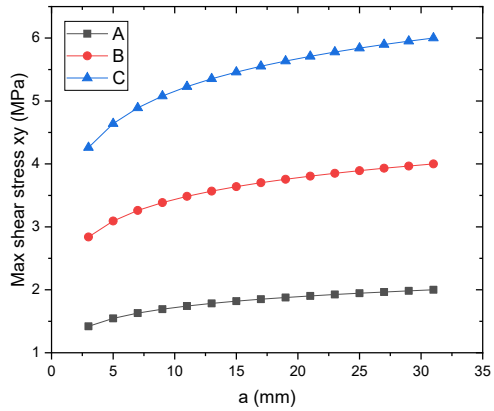

Fig. 13. Effect of the different stacking sequences on the maximum shear stresses (xy) in the adhesive layer

Fig. 14 focuses on the shear stress in the (xz) plane. Sequence [A] starts with an initial maximum shear stress of approximately 7.10 MPa and experiences a steady increase throughout the loading, eventually reaching close to 10.00 MPa. Sequence [B] initiates with a higher shear stress of around 14.19 MPa and follows a similar pattern of continuous growth, culminating at approximately 20.00 MPa. In contrast, sequence [C], which is meant to be studying the shear stress in the (xy) plane, exhibits significantly higher values throughout, starting at approximately 21.29 MPa and progressing to about 30.00 MPa. These data indicate that the FM-73 adhesive's shear behavior in the (xz) plane, as represented by sequences [A] and [B], demonstrates lower shear resistance compared to that in the (xy) plane, as represented by sequence [C]. Further investigations are required to comprehend the underlying factors contributing to these differences and their implications for the adhesive's application in shear loading scenarios.

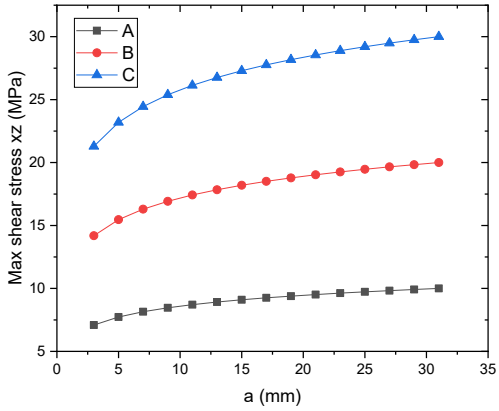

Fig. 14. Effect of the different stacking sequences on the maximum shear stresses (xz) in the adhesive layer

In the examination of FM-73 shear adhesive's response to shear loading, with a focus on maximum shear stress values in the (yz) plane, Fig. 15 shows a clear progression in the three loading sequences, denoted as [A], [B], and [C]. Sequence [A] starts with an initial maximum shear stress of approximately 23.65 MPa and shows a consistent increase throughout the loading process, reaching nearly 33.33 MPa. Sequence [B], beginning with a higher shear stress of around 47.30 MPa, also exhibits a continuous growth pattern, culminating at approximately 66.67 MPa. Notably, sequence [C], intended to explore shear stress in the (yz) plane, maintains significantly higher values throughout the experiment, commencing at approximately 70.95 MPa and progressing to about 100.00 MPa. These data underscore that FM-73 shear adhesive demonstrates a substantial shear strength in the (yz) plane, as represented by sequence [C], which is significantly greater than the shear strengths observed in the (xz) plane (sequences [A] and [B]).

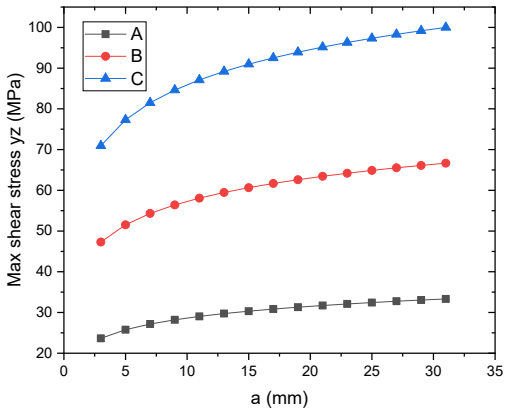

Fig. 15. Effect of the different stacking sequences on the maximum shear stresses (yz) in the adhesive layer

7. Conclusion

Our comprehensive discussions explore the detailed functioning of repair patches and finite element modeling, revealing insights into the subtle dynamics of stress intensity factors K1 and K2. The effectiveness of repair sequences, particularly under diverse shear conditions, was underscored, emphasizing their pivotal role in enhancing structural integrity. Additionally, our exploration of finite element modeling revealed the critical relationship between mesh refinement and accurate stress predictions, emphasizing the need for precision in modeling techniques. On a parallel note, the analysis of FM-73 adhesive brought to the forefront its dynamic behavior under distinct loading conditions and strain scenarios. Notably, sequence [A] emerged as consistently delivering the highest shear resistance, with the adhesive showcasing superior strength in the (yz) plane. The nonlinear stress-strain relationship of FM-73 further accentuates its versatile nature, poised for tailored applications through a nuanced understanding of its responses. Collectively, these insights propel advancements in materials science and structural engineering, providing practical guidance for optimizing repair strategies and harnessing the potential of FM-73 adhesive in diverse engineering and bonding applications.

References

A. Baker (1995). Bonded composite repair of metallic aircraft components overview of Australian activities, AGARD-CP-550, pp. 1-14.

A. Baker (1984). Repair of cracked or defective metallic aircraft components with advanced fiber composites-an overview of Australian work. J. Compos. Struct. 2, 153–8.

A. Benkheira et al. (2022). Experimental and Numerical Study of the Effect of Debonding Defect in Composite Patch Repairs on Composite Plate, J Fail. Anal. and Preven. 22:1669–169 https://doi.org/10.1007/s11668-022-01455-0

Abaqus Simulia, Dassault Systems. Abaqus software. Version 6.14. (2014).

Bouchiba, S. and Serier, B. (2016). New optimization method of patch shape to improve the effectiveness of cracked plates repair. Structural Engineering and Mchanic. 58(2), pp. 301-326. DOI: 10.12989/sem.2016.58.2.301.

Chung, K.H. and Yang, W.H. (2003). A study of the fatigue crack growth behavior of thick aluminum panels repaired with composite patch. Composite Structures.60. pp. 1-7. DOI: 10.1016/S0263-8223(02)00095-8.

Chung, K.H., Yang, W.H. and Cho, M.R. (2000). Fracture mechanics Analysis of cracked Plate Repaired by Composite Patch. Key Engineering Material, 43-8, pp. 183-187. DOI: 10.4028/www.scientific.net/KEM.183-187.43.

D. C. Seo, J. J. Lee (2002). Fatigue crack growth behavior of cracked aluminum plate repaired with composite patch, Compos. Struct. 57(1) 323-330.

F. Benyahia, A. Albedah, B. Bachir Bouiadjra (2014). Analysis of the adhesive damage for different patch shapes in bonded composite repair of aircraft structures. Mater. Des. 1980–2015(54), 18–24.

J Salem et al. (2021). Analysis of the Adhesive Damage for Different Patch Shapes in Bonded Composite Repair of Corroded Aluminum Plate Under Thermo-Mechanical Loading J Fail. Anal. and Preven. 21:1274–1282 https://doi.org/10.1007/s11668-021-01167-x

Jeong, G.H.Y., Won-Ho, Jo. and Myeong, Rae. (2000). Fracture Mechanics Analysis of Cracked Plate Repaired by Patch (I). Transaction of the Korean Society of Material Engineers 24 (8), pp. 2000-2006. DOI: 10.22634/KSME-A.2000.24.8.2000.

Luzar, J. J. (1997). Pre-corroded Fastener Hole Multiple Site Damage Testing, Final Report, EA 96-135OTH-041, Boeing ISDS Post-Production/Derivative Aircraft Division, December 1997.

M. Berrahou, M. Salema, M. Mechab, B.B. Bouiadjrab (2017). Effect of the corrosion of plate with double cracks in bonded composite repair. Struct. Eng. Mech. 64, 323–328.

M. R. Ayatollahi, R. Hashemi (2007). Computation of stress intensity factors (K I, K II) and Tstress for cracks reinforced by composite patching, Compos. Struct. 78(4) 602-609.

M. Salem, M. Berrahou, B. Mechab, B. Bachir Bouadjra (2018). Effect of the angles of the cracks of corroded plate in bonded composite repair. Frattura ed Integrita` Strutturale. 46, 113–123.

M. Salem, M. Berrahou, B. Mechab, B.B. Bouiadjra (2021). Analysis of the adhesive damage for different patch shapes in bonded composite repair of corroded aluminum plate under thermomechanical loading. J. Fail. Anal. Prev. 21, 1274–1282.

Mechab B, Medjahdi M, Salem M, Serier B (2020). Probabilistic elastic - plastic fracture mechanics analysis of propagation of cracks in pipes under internal pressure, Frattura Ed Integrita Strutturale, 14(54). pp. 202-210.

Mhamdia, R., Serier, B., Bachir Bouiadjra, B. and Belhouari, M. (2012). Numerical analysis of the patch shape effects on the performances of bonded composite repair in aircraft structures. Composites: Part B, 43, pp. 391–397. DOI:10.1016/j.compositesb. 2011.08.047.

N.C.M. Ibrahim, B. Serier, B. Mechab (2018). Analysis of the crackcrack interaction effect initiated in aeronautical structures and repaired by composite patch. Frattura ed Integrita` Strutturale. 46,140–149.

Rose, L.R.F. (1981), “An application of the inclusion analogy for bonded reinforcements”, Int. J. Solid. Struct. 17, 827-38.

S.N. Atluri, Structural Integrity and Durability. (Tech Science Press, Forsyth, Georgia, USA, 1997)

T.N. Chakherlou and all Effect of cold expansion on the fatigue life of Al 2024-T3 in double shear lap joints: Experimental and numerical investigations Materials and Design 33 (2012) 185–196

W.T. Chow, S.N. Atluri, Composite patch repairs of metal structures: adhesive nonlinearity, thermal cycling, and debonding. AIAA J. 35(9), 1528–1535 (1997)